EFFECTS OF SEA SALTS ON THE PHYSICAL CHARACTERISTICS OF REUSABLE SURFACE INSULATION

By

Philip O. Ransone and Dennis L. Dicus

Langley Research Center

INTRODUCTION

(Figure 1)

The coatings on Reusable Surface Insulation (RSI) which are proposed for space shuttle are formulated of ceramic phases that can be modified by contamination with light metal salts contained in sea water. Since Cape Kennedy has been chosen as a base for space shuttle, it is important to determine if RSI coatings will be affected by exposure to the coastal atmosphere, which contains measurable quantities of sea salts.

Compositional changes of the glass in RSI coatings resulting from contamination with sea water salts are likely to modify melting temperature, melt viscosity, and thermal expansion. Changes in composition can influence the behavior of existing crystalline phases as well. In the silica glass system, contaminate particles can act as nucleation sites for devitrification. The resulting cristobalite phase can be destructive in a thermal cyclic environment because of the volume changes associated with polymorphic transformation of cristobalite. Since these coatings are designed to provide high emittance, the effect on emittance of changes in the surface characteristics due to melting and crystallization must be examined.

This paper reports partial results of a preliminary study in which coated specimens of RSI were exposed to sea salt and radiant heat cycles in the laboratory. The intent of this study was to demonstrate the necessity for testing these materials under realistic environmental conditions.

EFFECT OF SEA SALTS ON RSI COATINGS DURING REENTRY HEATING

- MELTING TEMPERATURE AND MELT VISCOSITY LOWERED
- CRYSTALLINE PHASE CHANGES
- EXPANSION CHANGES, VOLUME AND THERMAL
- POSSIBLE EMITTANCE CHANGES DUE TO CHANGES IN SURFACE CHARACTERISTICS

Figure 1

MATERIALS

(Figure 2)

Test specimens were cut to dimensions 3.2 cm square by 2.5 cm thick from large coated tiles of each material listed in this figure. One face of each specimen was coated.

The McDonnell Douglas (MDAC) material is coated with a base coat $M5_{23}$, a phosphate bonded chromium oxide diffusion barrier A, a borosilicate seal coat 7, and a P_{700} emittance agent containing iron, cobalt, and chromium oxides. The insulation is mullite fiber with silica microspheres and silica binder.

The coating on the General Electric (GE) material is a kyanite/petalite multiphase glass composition with a nickel oxide emittance agent. The insulation is mullite fiber with Al_2O_3–SiO_2–B_2O_3 glass binder.

The coating on the Lockheed (LMSC) material is a borosilicate glass with a silicon carbide emittance agent dispersed in the glass. The insulation is silica fiber with collodial silica binder.

The thickness of the coatings on all materials is nominally 0.038 cm. The GE and LMSC coatings are considered current baseline, but the MDAC coating has been superseded by a newer version, MM_p P_{Cr} $7P_{700}$.

MATERIALS

COMPANY	COATING DESIGNATION	INSULATION DESIGNATION
MDAC	$M5_{23}A7P_{700}$	MULLITE-HCF MOD III
GE	SR-2	REI MULLITE MOD I-A
LMSC	LI-0042	LI-1500

Figure 2

TEST PROCEDURE

(Figure 3)

This figure depicts the test procedure followed in this investigation. Specimens were alternately exposed to sea water fog and temperature cycles up to 50 times. Sea water was applied to specimens as an atomized spray. The weight of solids deposited per application was 0.05 - 0.08 mg/cm^2. Additional specimens were subjected to the same number of temperature cycles but without contamination. The temperature cycle used was a radiant heat simulation of short cross-range re-entry. The test cycle was 2700 sec reaching a maximum of 1530°K at 1700 sec but with a hold at 1140°K for most of the first 1550 sec. After completion of the cyclic heating and salt exposure, X-ray diffraction patterns were obtained for all specimens by scanning the coating surface at $2\theta = 2°/min$ with Nickel filtered Cu Kα radiation. Crystalline phases were identified by comparing d-spacings and intensities of the measured patterns with the ASTM powder diffraction file.

Spectral emittance of specimens was measured in the 1-15 μm range at temperatures of 800°, 1100°, and 1300°K using the method described by Kantsios et al. in Volume I of these Proceedings. Total normal emittance was calculated from these data by integrating over the wavelength. Specimens were then prepared for photographic documentation and destructive analyses.

TEST PROCEDURE

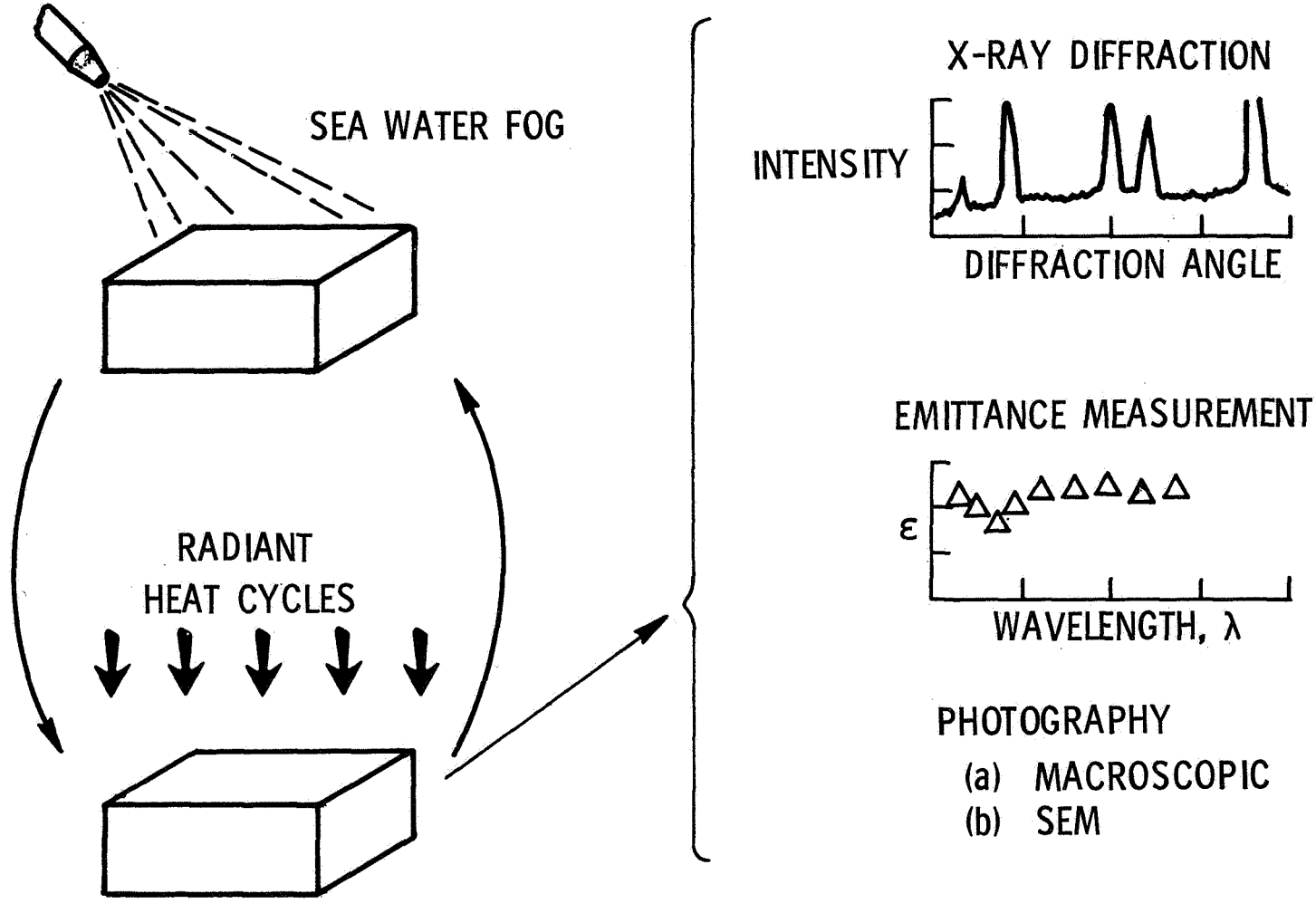

Figure 3

X-RAY DIFFRACTION PATTERNS OF $M5_{23}A7P_{700}$ COATING

(Figure 4)

This figure shows X-ray diffraction patterns for the MDAC coating in the as-received condition and after 50 thermal cycles with and without sea salt contamination. The contaminated specimen was sprayed with sea water before each of the 50 thermal cycles. Chromium oxide was the only crystalline phase identified in this coating. No new phases appeared after 50 cycles with or without contamination; however, there was some reduction in the amount of phase present as indicated by weakening of the diffraction lines.

X-RAY DIFFRACTION PATTERNS OF $M5_{23}A7P_{700}$ COATING

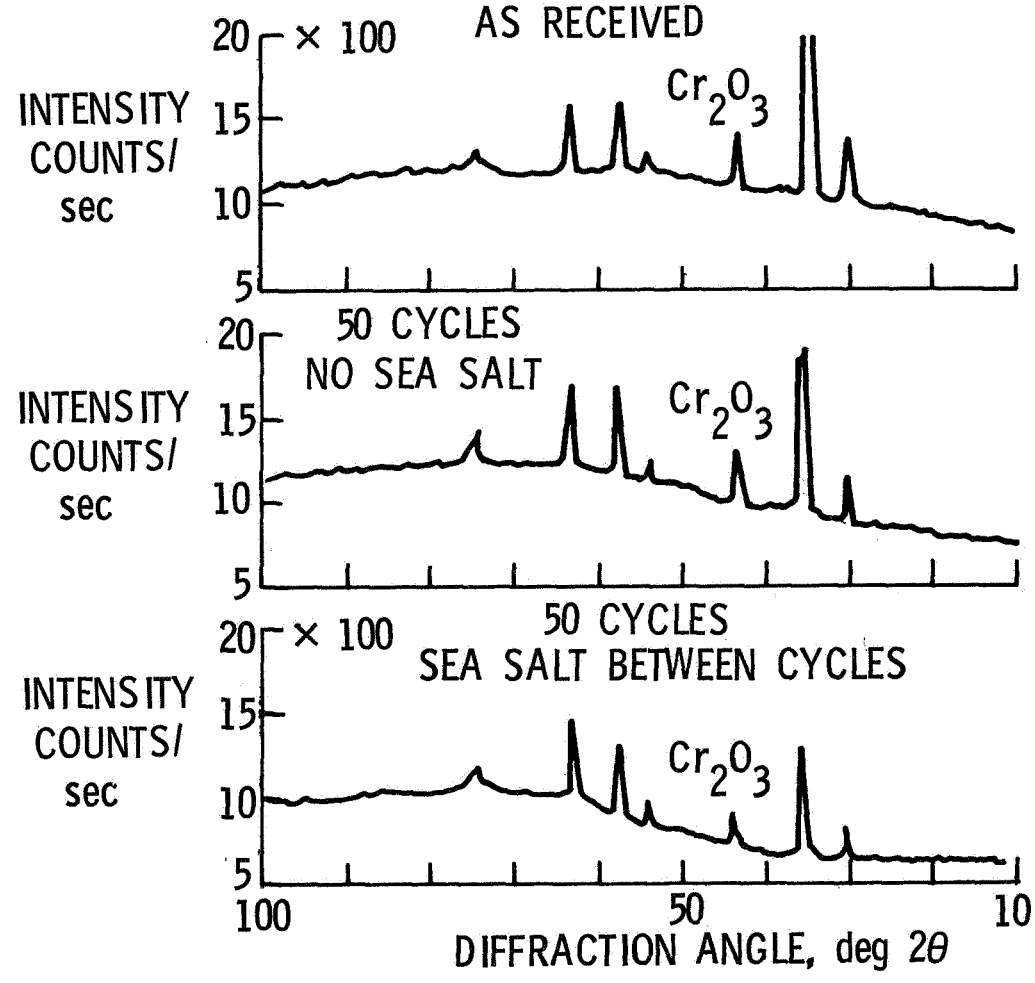

Figure 4

X-RAY DIFFRACTION PATTERN OF SR-2 COATING

As Received

(Figure 5)

This figure shows an X-ray diffraction pattern of the G.E. coating in the as-received condition. Three crystalline phases were tentatively identified in this coating. The strongest lines belong to the μ cordierite phase. Remaining lines agree closely with the lines of Iota alumina and nickel aluminate spinel.

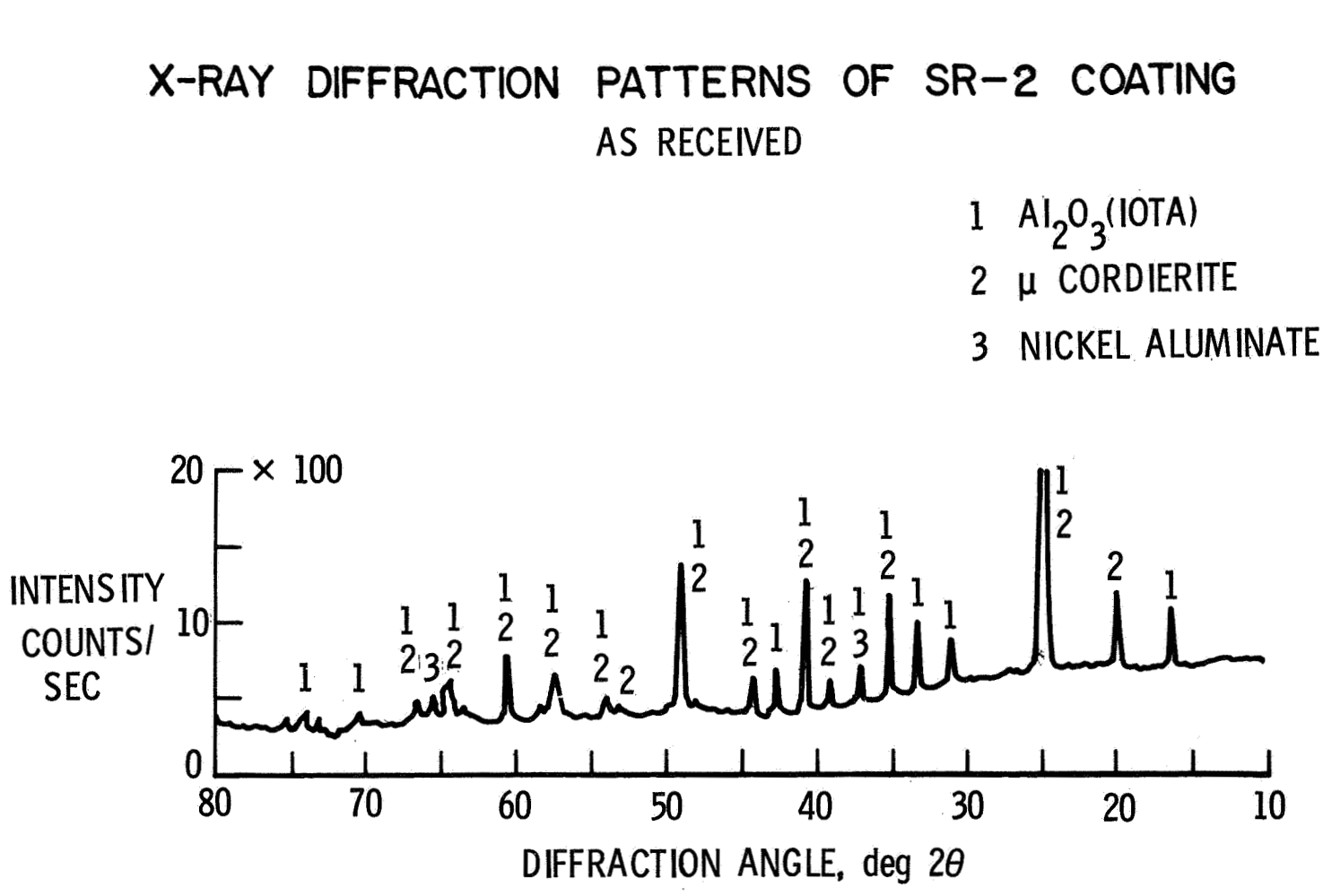
X-RAY DIFFRACTION PATTERNS OF SR-2 COATING
AS RECEIVED
1 Al_2O_3(IOTA)
2 μ CORDIERITE
3 NICKEL ALUMINATE
INTENSITY COUNTS/ SEC
20
× 100
10
0
80
70
60
50
40
30
20
10
DIFFRACTION ANGLE, deg 2θ

Figure 5

X-RAY DIFFRACTION PATTERNS OF SR-2 COATING

50 Thermal Cycles

(Figure 6)

Shown in this figure are X-ray diffraction patterns of contaminated and uncontaminated G.E. specimens after 50 thermal cycles. The contaminated specimen was sprayed with sea water before every cycle. When comparing the patterns in this figure to those of figure 5, it is seen that thermal cycles initiate a cristobalite phase and that contamination with salt inhibits initiation of the cristobalite phase. Contamination greatly accelerates the growth of the nickel aluminate phase but causes the cordierite and alumina phases to be dissolved.

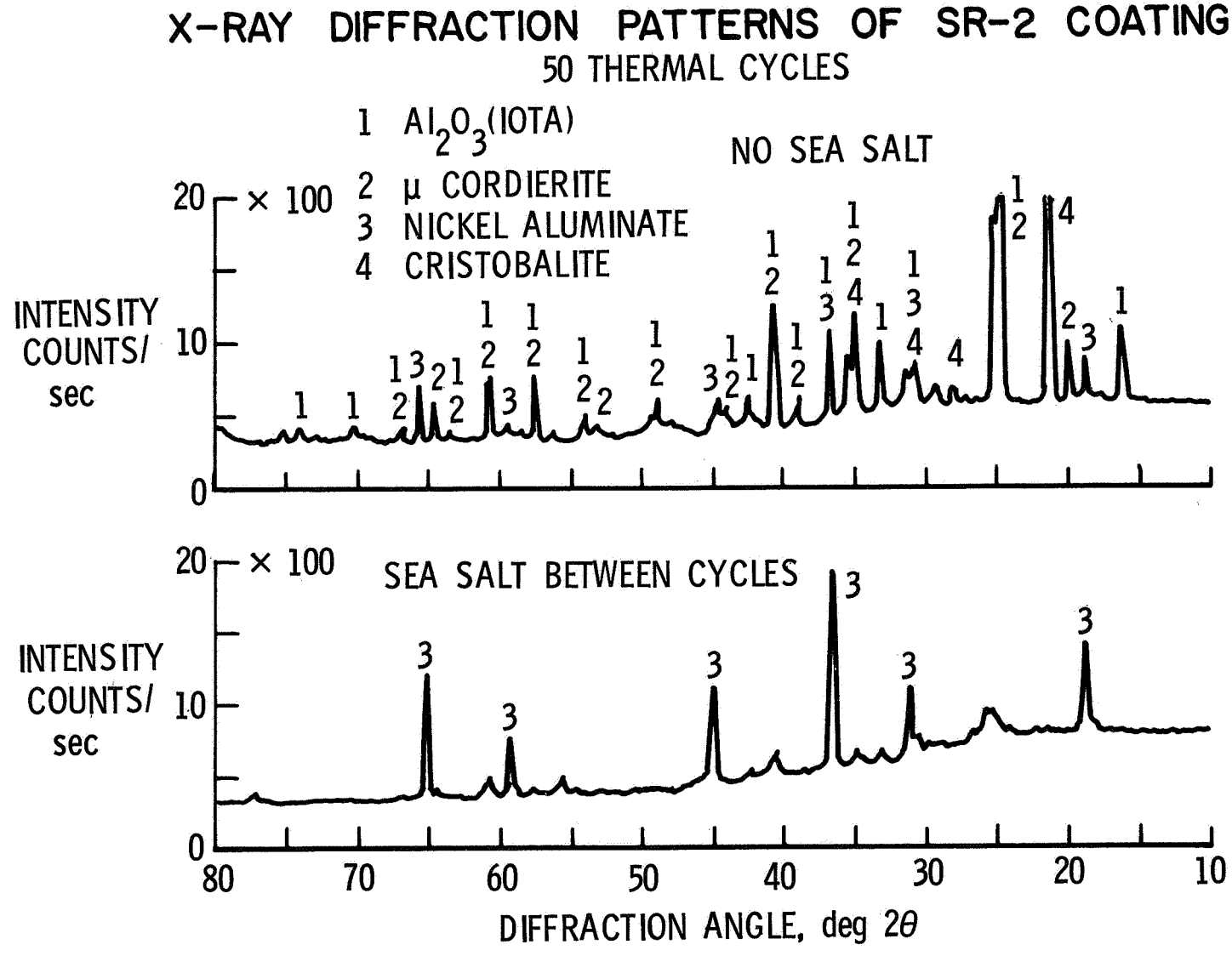
X-RAY DIFFRACTION PATTERNS OF SR-2 COATING
50 THERMAL CYCLES
1 Al_2O_3(IOTA)
2 μ CORDIERITE
3 NICKEL ALUMINATE
4 CRISTOBALITE
NO SEA SALT
SEA SALT BETWEEN CYCLES
× 100
INTENSITY COUNTS/ sec
20
10
0
80
70
60
50
40
30
20
10
DIFFRACTION ANGLE, deg 2θ

Figure 6

X-RAY DIFFRACTION PATTERNS OF LI-0042 COATING
As Received
(Figure 7)

This figure shows X-ray diffraction patterns of the LMSC coating in the as-received condition and after 10 thermal cycles with and without contamination. The contaminated specimen was sprayed with sea water before the first cycle only. Silicon carbide was the only cyrstalline phase identified in the as-received coating. After 10 thermal cycles, the effect of contamination on cristobalite growth is apparent.

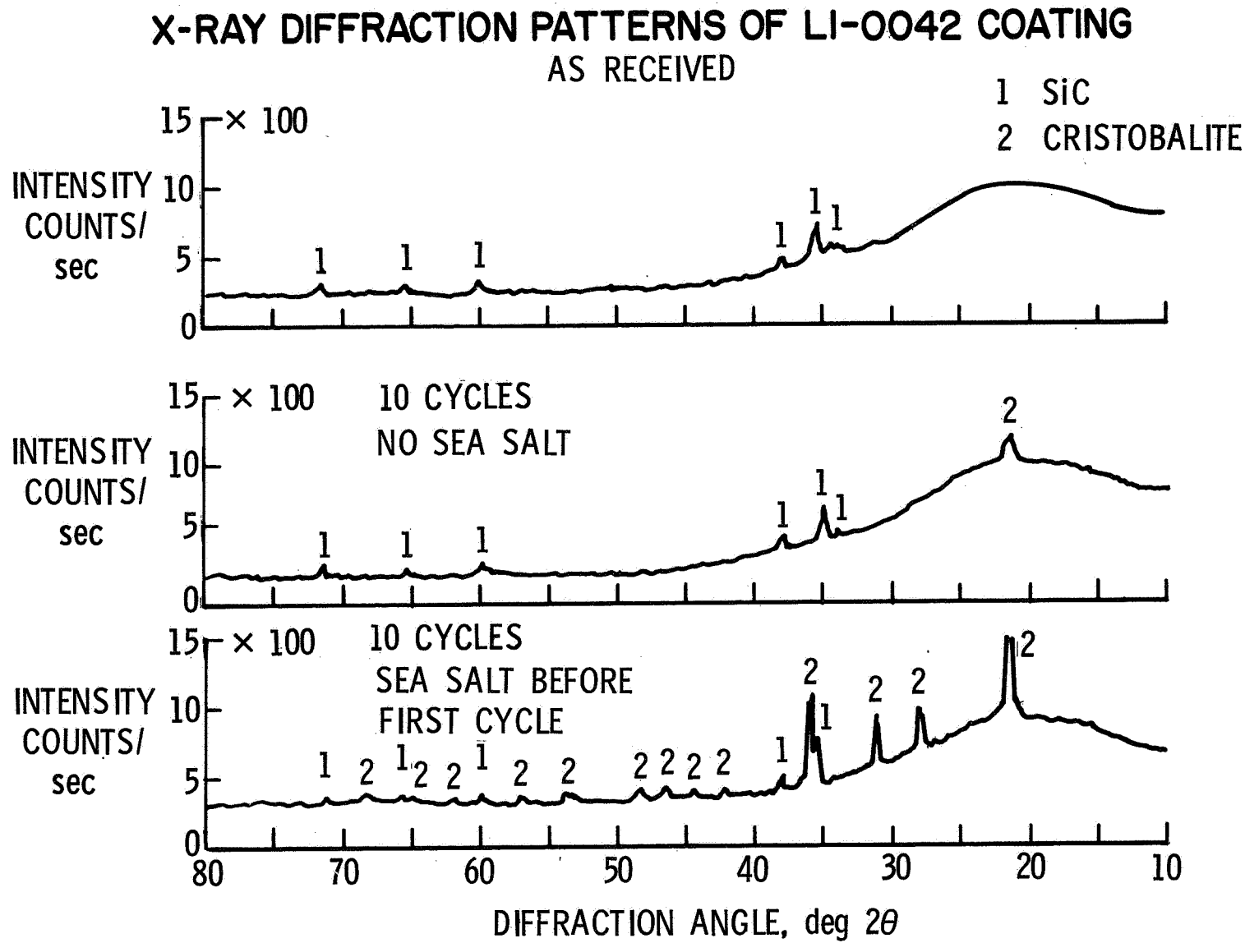
X-RAY DIFFRACTION PATTERNS OF LI-0042 COATING
AS RECEIVED
1 SiC
2 CRISTOBALITE
INTENSITY COUNTS/ sec
15
× 100
10
5
0
10 CYCLES
NO SEA SALT
10 CYCLES
SEA SALT BEFORE
FIRST CYCLE
80
70
60
50
40
30
20
10
DIFFRACTION ANGLE, deg 2θ

Figure 7

X-RAY DIFFRACTION PATTERNS OF LI-0042 COATING

50 Thermal Cycles

(Figure 8)

The X-ray diffraction patterns shown in this figure are of the LMSC coating after 50 thermal cycles. No sea water was sprayed on the specimen that produced the first pattern. The specimens that produced the next two patterns were sprayed with one and four applications, respectively. These data show that there is a definite acceleration of devitrification associated with degree of sea salt contamination.

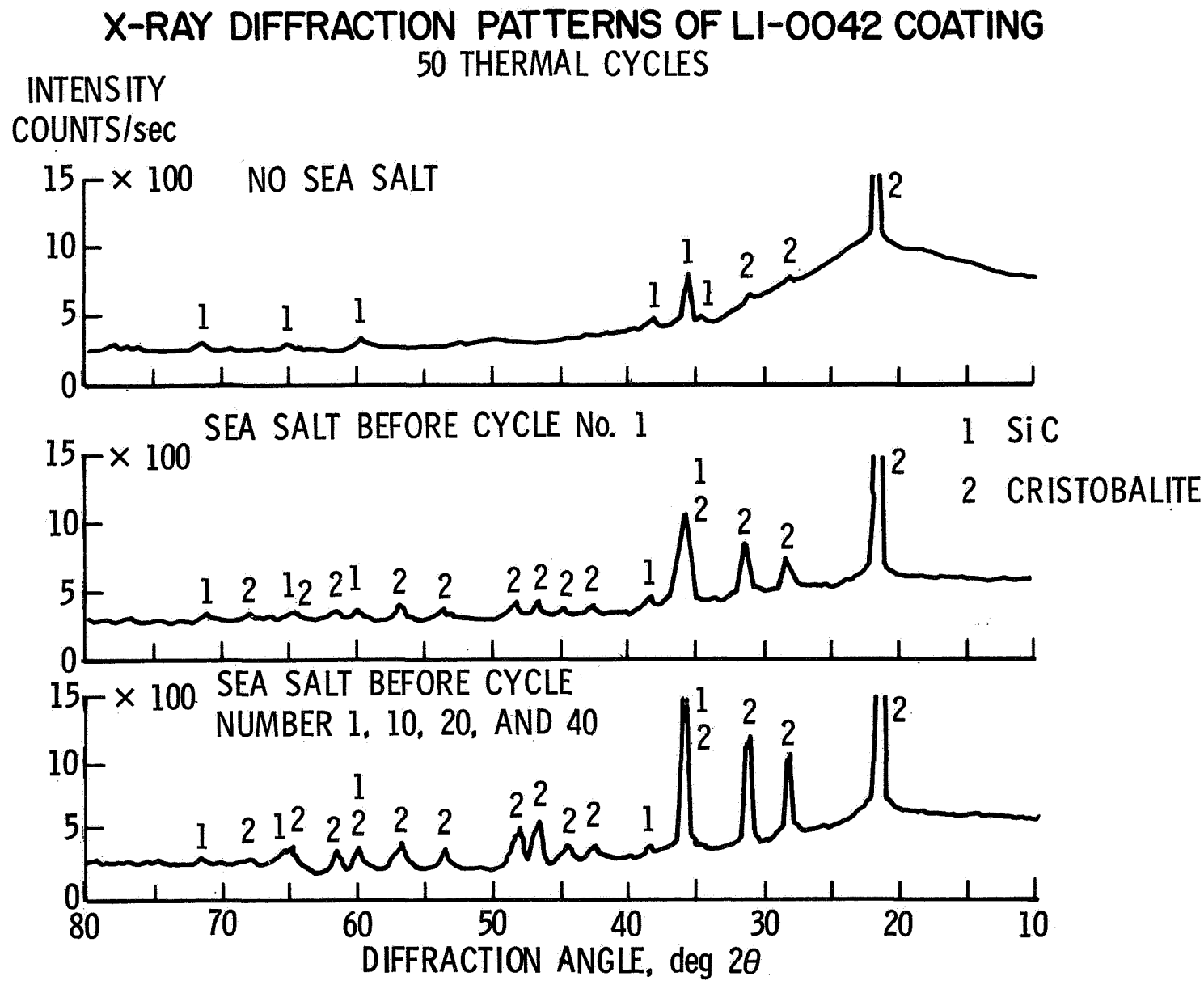
X-RAY DIFFRACTION PATTERNS OF LI-0042 COATING
50 THERMAL CYCLES
INTENSITY
COUNTS/sec
15
× 100
NO SEA SALT
10
5
0
SEA SALT BEFORE CYCLE No. 1
SEA SALT BEFORE CYCLE
NUMBER 1, 10, 20, AND 40
1 SiC
2 CRISTOBALITE
80
70
60
50
40
30
20
10
DIFFRACTION ANGLE, deg 2θ

Figure 8

X-RAY DIFFRACTION PATTERNS OF LI-0042 COATING

20 Thermal Cycles + Sea Salt Between Cycles

(Figure 9)

The diffraction patterns shown in this figure were obtained to pinpoint the origin(s) of cristobalite formation in a LMSC specimen after contamination and thermal cycles. This was necessary because of suspicion that cristobalite was being detected in the insulation through cracks in the coating. The top pattern was obtained from a piece of coating that was removed from the specimen, mounted, and polished to remove traces of insulation from the backside. The resulting lines in the pattern must therefore belong to cristobalite originating in the coating. The lower pattern was obtained before removing the piece of coating from the specimen. This pattern shows stronger cristobalite lines which suggests that some cristobalite in the insulation is contributing to the intensities of the lines by means of X-rays passing through cracks in the coating. The existence of cracks in the coating is verified in the photograph of this test specimen shown in figure 10.

X-RAY DIFFRACTION PATTERNS OF LI-0042 COATING

20 THERMAL CYCLES + SEA SALT BETWEEN CYCLES

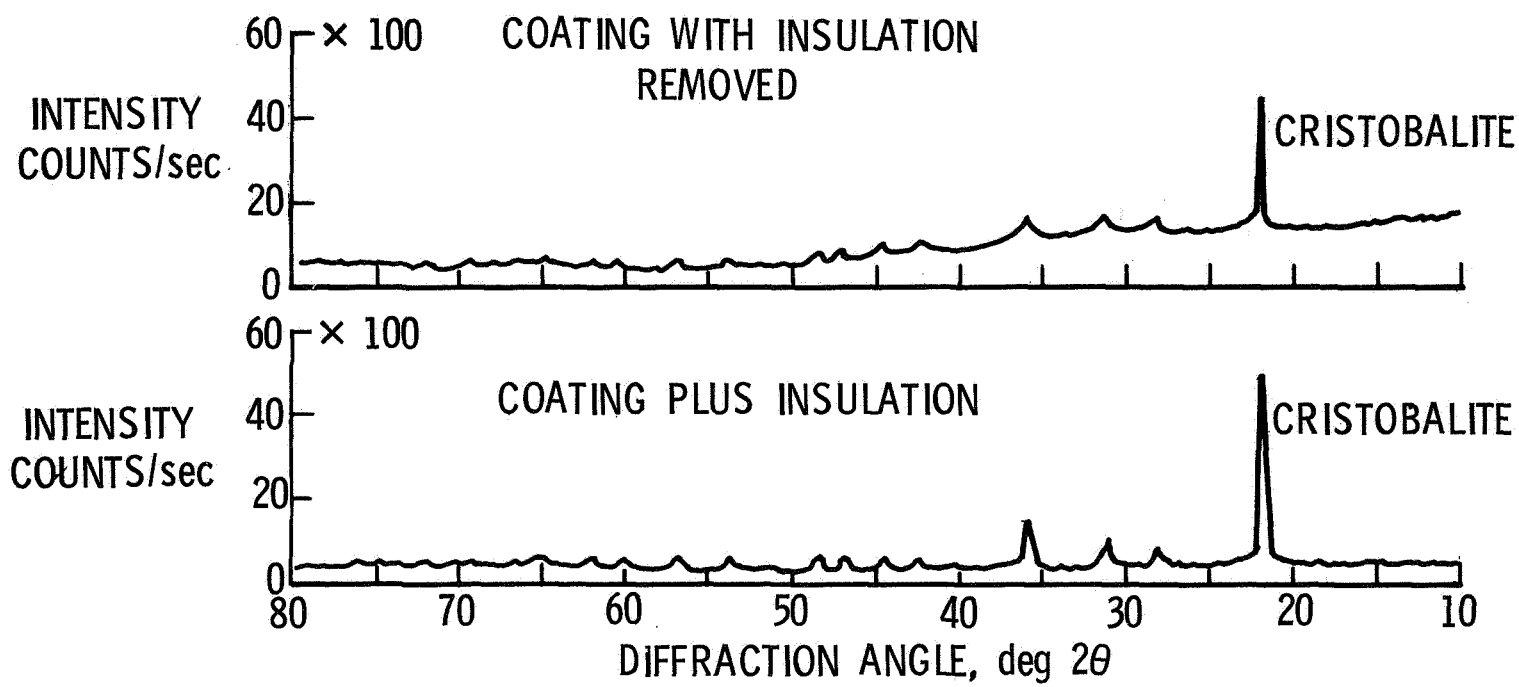

Figure 9

PHOTOGRAPHS OF THERMAL CYCLIC TESTS ON RSI SPECIMENS

(Figure 10)

This figure shows photographs of tested and as-received specimens. Increased melting as a result of sea salt contamination is apparent in the MDAC and GE coatings. There is apparently no melting of the LMSC coating, but several cracks are visible in the 20 cycle specimen (same specimen discussed in figure 9). This specimen was one of three that were contaminated before each cycle. In all cases, the coating cracked. These specimens were not instrumented with thermocouples because they induced cracking in earlier 10 cycles tests. Cracking is thought to be associated with the polymorphic transformation of cristobalite during thermal cycling.

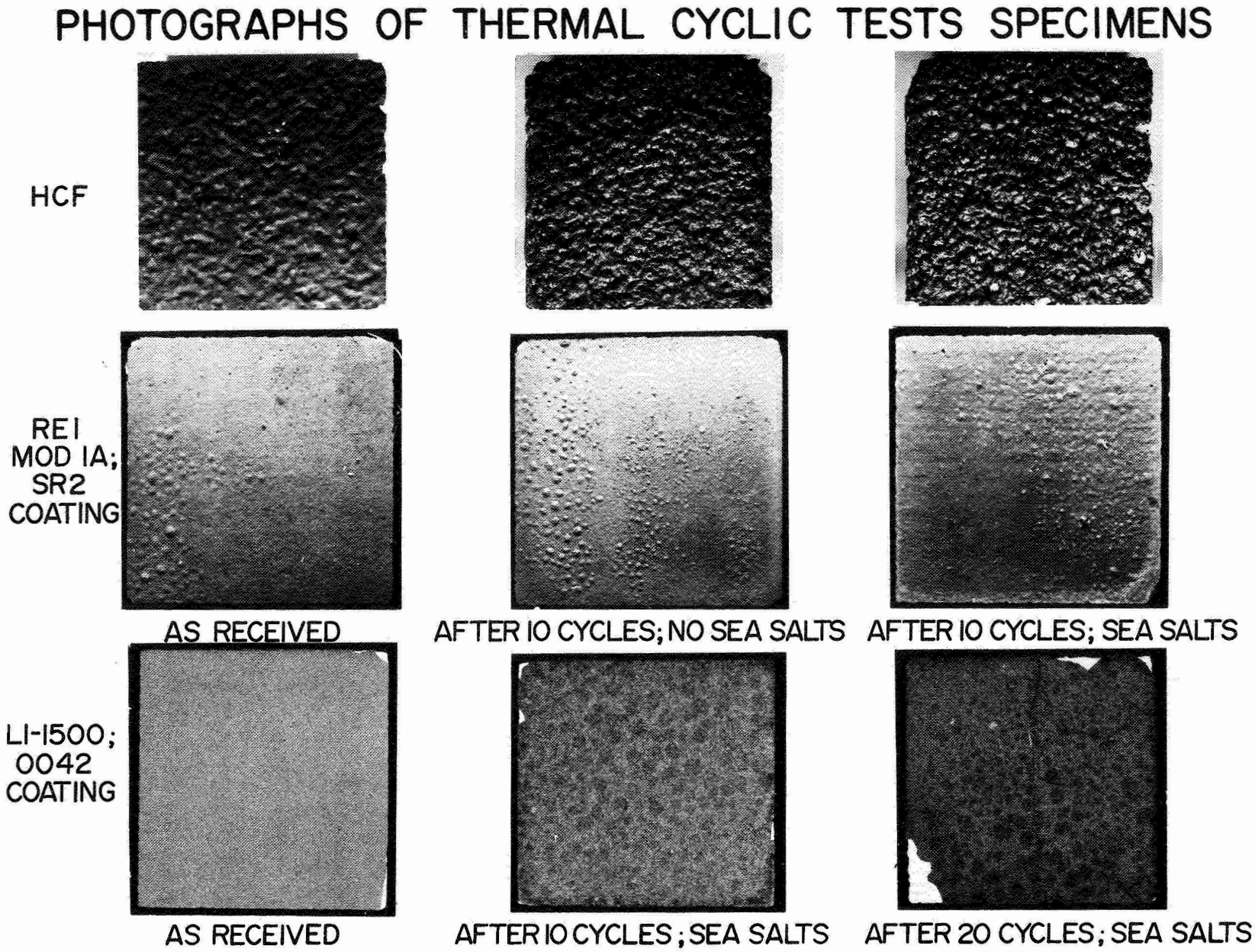
PHOTOGRAPHS OF THERMAL CYCLIC TESTS SPECIMENS
HCF
REI MOD IA; SR2 COATING
LI-1500; 0042 COATING
AS RECEIVED
AFTER 10 CYCLES; NO SEA SALTS
AFTER 10 CYCLES; SEA SALTS
AS RECEIVED
AFTER 10 CYCLES; SEA SALTS
AFTER 20 CYCLES; SEA SALTS

Figure 10

EFFECT OF SEA SALT AND THERMAL CYCLES ON EMITTANCE OF $M5_{23}A7P_{700}$ COATING

(Figure 11)

This figure shows total normal emittance versus temperature for MDAC specimens. The as-received data points are average values based on readings from three different specimens. The bars show the range of as-received values. The 50 cycle data are based on measurements from single specimens, thus making any accurate interpretation of the 50 cycle data difficult. The as-received data show a drop in emittance with increasing temperature. The 50 cycle data show little effect at the high temperature but possibly some decrease in emittance at the low temperature because of contamination. The reader is reminded that the contaminated specimen was exposed to salt before each cycle.

EFFECT OF SEA SALT AND THERMAL CYCLES ON EMITTANCE OF $M5_{23}A7P_{700}$ COATING

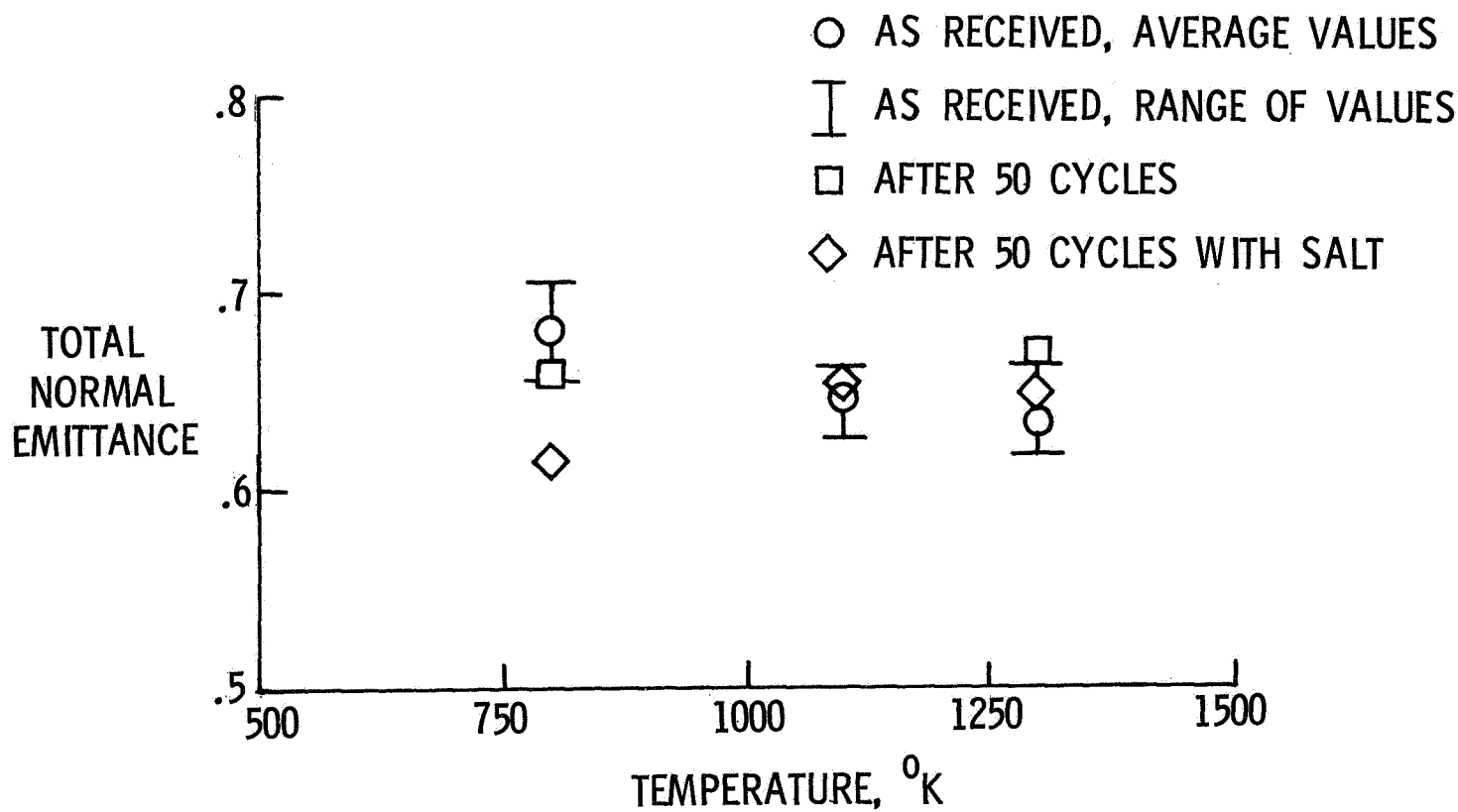

Figure 11

EFFECT OF SEA SALT AND THERMAL CYCLES ON EMITTANCE OF SR-2 COATING

(Figure 12)

This figure presents total normal emittance versus temperature data for the G.E. specimens. Again, the as-received data are based on measurements from three specimens and the 50 cycle data from single specimens. The as-received coating shows a drop in emittance with increasing temperature from a value higher than that of the MDAC coating to about an equal value ($\approx$ .65). Thermal cycles and contamination show little effect on emittance at the high temperature, but there is a distinctive difference at the low temperature. In this case, contamination appears to have tempered the effect of thermal cycles. Again, the reader is reminded that the contaminated specimen was exposed before each cycle.

EFFECT OF SEA SALT AND THERMAL CYCLES ON EMITTANCE OF SR-2 COATING

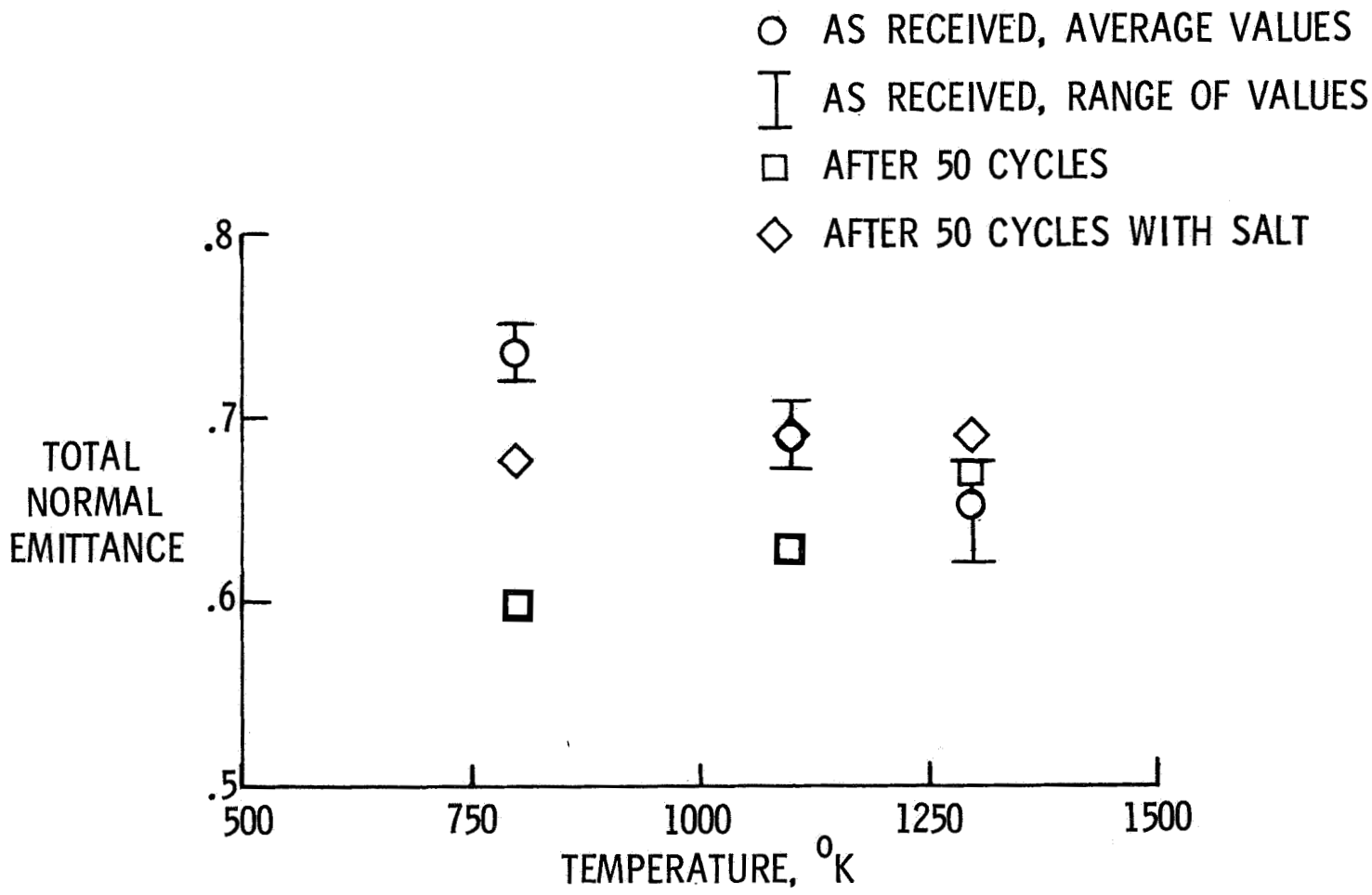

Figure 12

EFFECT OF SEA SALT AND THERMAL CYCLES ON EMITTANCE OF LI-0042 COATING

(Figure 13)

Total normal emittance versus temperature data are presented in this figure for LMSC specimens. The average as-received values are based on measurements from five specimens and the 50 cycle data from single specimens. Note the wider range of as-received values for the middle and lower temperatures. Emittance drops with temperature to a value of .63 or about equal to the other two materials at the high temperature. Thermal cycles appear to have some effect on emittance at the lower temperatures but, as with the other materials, show very little influence at the high temperature. In this case, contamination has shown no effect over the range of temperatures. It should be noted that the contaminated specimen was subjected to only four salt exposures where the other materials were exposed 50 times. Data could not be obtained from a 50 cycle specimen of the LMSC material after 50 salt exposures because of disintegration of the coating.

EFFECT OF SEA SALT AND THERMAL CYCLES ON EMITTANCE OF LI-0042 COATING

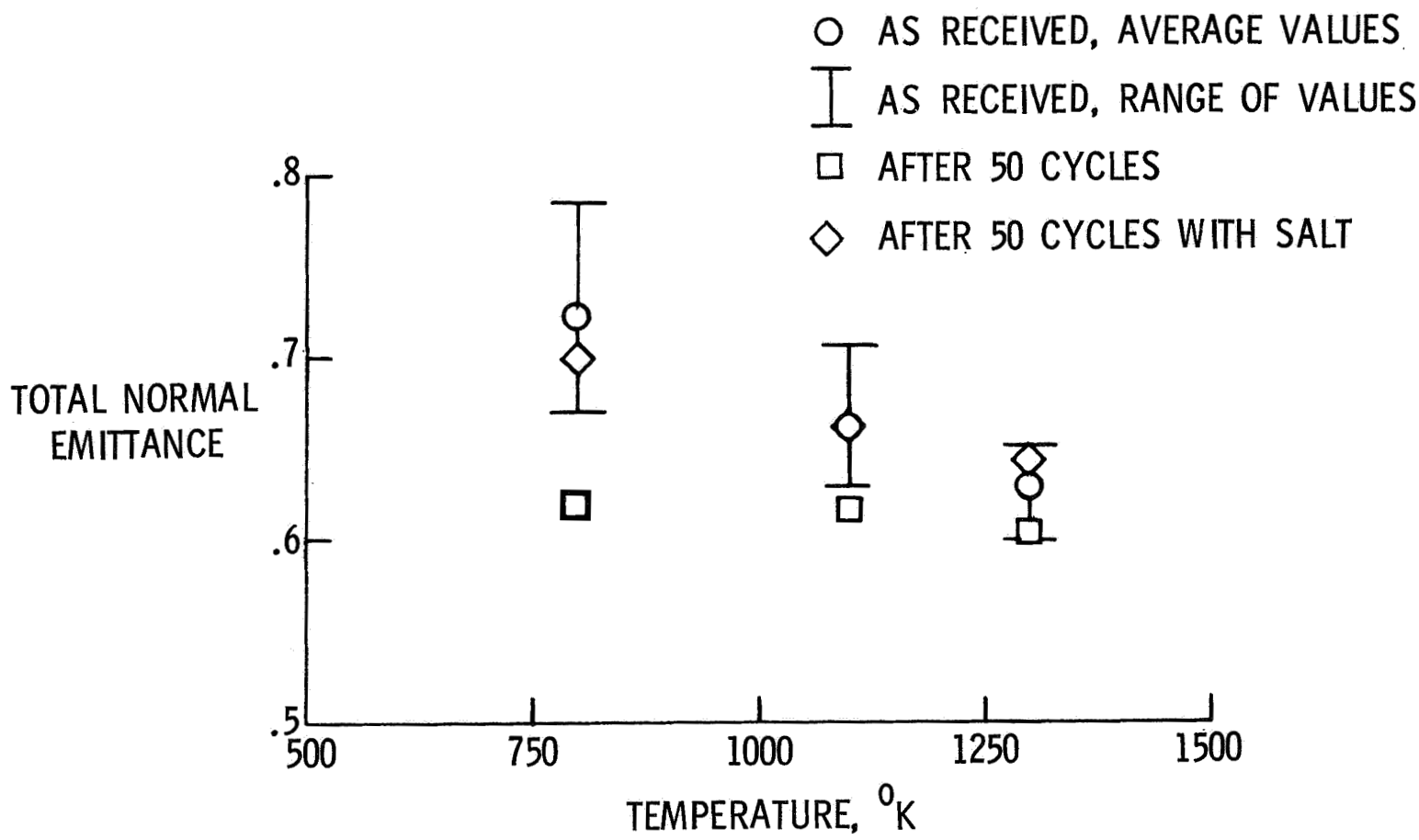

Figure 13

SUMMARY REMARKS

Results of this investigation show that sea salt contamination and thermal cycles cause significant changes in the morphology of the LMSC and GE coatings. Contamination causes increased melting of the GE and MDAC coatings. Sea salt contamination and thermal cycles do not have a significant effect on emittance of either coating at high temperatures (1300°K). At the lower temperatures there is apparently some effect on emittance but the evidence is inconclusive because of the absence of multiple tests.

STATUS

Emittance data, to date, have been obtained from a limited number of specimens because of a limited supply of material. More tests are needed on large numbers of specimens to conclusively determine the effects of thermal cycling and contamination on emittance.

Results of this investigation have led to the initiation of a joint program between Langley Research Center and Kennedy Space Center. In this program, coatings will be exposed to actual environmental conditions and realistic thermal testing.